RSC Advances

PAPER

View Article Online
View Journal | View Issue

Open Access Article. Published on 12 August 2025. Downloaded on 1/21/2026 11:52:35 PM.
This article is licensed under a Creative Commons Attribution-NonCommercial 3.0 Unported Licence.

Check for updates

Cite this: *RSC Adv.*, 2025, **15**, 28464

Process intensification of anaerobic digestion for biohydrogen and methane production from crude glycerol and dairy wastewater using cavitation techniques

Mohd Mohsin Ikram,[a] Jitendra Carpenter *[b] and Virendra Kumar Saharan *[a]

This study investigates methane production from the mono-digestion of dairy wastewater (DWW) and hydrogen production from the co-digestion of DWW and crude glycerol (CG), both of which are abundantly available in India. In this study, ultrasonication (US) and hydrodynamic cavitation (HC) were employed as pretreatment methods for DWW prior to mono and co-anaerobic digestion, with the aim of enhancing methane and hydrogen production. The results show that these methods significantly improve methane yield, offering a sustainable solution for efficient bioenergy recovery from organic waste. The highest methane yield from DWW was achieved using US at an amplitude of 60% and a treatment duration of 30 min, resulting in a maximum cumulative methane yield (P_{max}) of 413 mL, with a production rate (r_m) of 26.31 mL per day and a lag phase (λ) of 23.19 days. In a similar experiment, treating DWW with HC using a venturi with a 2 mm hole size, the P_{max} was 341.21 mL at a pressure of 5 bar and a treatment time of 30 min. This process resulted in a r_m of 24.43 mL per day and a λ of 29.74 days. Additionally, when CG was combined with DWW, the maximum cumulative hydrogen yield reached 330.8 mL at a 4% v/v concentration of CG, with r_m of 45.6 mL per day and a λ of 0.69 days. At CG concentrations ranging from 0.2 to 1% v/v, both hydrogen and methane were produced. However, beyond a 1% v/v CG concentration, methane production began to decrease. It was also found that pretreatment using HC and US did not enhance hydrogen production when CG was co-digested with pretreated DWW. These findings highlight the potential of integrating US, HC, and co-digestion strategies to enhance biofuel yields, promoting sustainable waste management and renewable energy solutions.

Received 10th June 2025
Accepted 3rd August 2025

DOI: 10.1039/d5ra04093k

rsc.li/rsc-advances

1 Introduction

The production of waste is an inevitable part of any industry, and the proper handling and disposal of waste and residues have become urgent issues in today's world. This necessitates the development of waste valorisation-focused management systems that incorporate sustainable and circular economy concepts. While numerous types of waste are being explored for valorisation, dairy waste has emerged as an important candidate due to its composition and availability. In a country like India, the largest producer of milk in the world, contributing 23% of global milk production,[1] the dairy industry has experienced remarkable growth in recent decades, leading to a significant increase in the waste generated by the sector. Dairy wastewater (DWW) is produced in large quantities, primarily from cleaning activities and leftover whey. This wastewater can be used in various beneficial applications, such as producing biofertilizers, biopolymers, and other valuable products, promoting sustainability and waste valorisation. DWW is a valuable resource due to its high organic load and cannot be discharged untreated. It can be converted into liquid biofertilizer[2,3] and combined with other carbon-rich sources, such as food waste,[4–7] to enhance biofuel production. Overall, DWW can be transformed into energy, especially through processes like biogas and biohydrogen production. In addition, these technologies promote sustainability by generating renewable energy and reducing dependency on fossil fuels.

Over the past three decades, biodiesel production has surged, leading to a significant increase in crude glycerol (CG) waste. For every 100 metric tonnes of biodiesel produced, approximately 10 metric tonnes of glycerol are generated.[8,9] To manage this substantial waste, it is essential to convert CG into value-added products. CG can be purified[10] and valorized into valuable products,[11,12] either directly[13] or by combining it with other waste streams for the generation of biohydrogen[14,15] and

[a]Department of Chemical Engineering, Malaviya National Institute of Technology, Jaipur 302017, Rajasthan, India. E-mail: vksaharan.chem@mnit.ac.in

[b]Department of Chemical Engineering, Manipal Institute of Technology, Manipal Academy of Higher Education, Manipal 576104, Karnataka, India. E-mail: jitendra.carpenter@manipal.edu

© 2025 The Author(s). Published by the Royal Society of Chemistry

Open Access Article. Published on 12 August 2025. Downloaded on 1/21/2026 11:52:35 PM.
This article is licensed under a Creative Commons Attribution-NonCommercial 3.0 Unported Licence.

biogas.[16,17] This approach addresses waste management challenges while contributing to renewable energy production and resource efficiency.

To enhance biogas production from raw materials, pretreatment techniques are often employed to improve the biodegradability of the substrate and reduce the λ, thereby increasing the r_m. Techniques like cavitation and heat treatment improve biogas production by dissolving sludge, biomass, and wastewater, thereby enhancing their biodegradability. Ultrasonication (US),[18] hydrodynamic cavitation (HC),[19] microwave treatment,[20] chemical treatment,[21] and ozonation[22] are examples of physicochemical techniques that enhance microbial access to substrates and facilitate the solubilization of organic materials. Biological approaches, such as enzymatic pretreatment,[23] microbial co-culturing,[24] and both aerobic[25] and anaerobic bioaugmentation,[26] are also used to maximize microbial activity and digestive efficiency. Mechanical techniques like high-pressure homogenization[27] and grinding/milling[28] increase surface area and decrease particle size, improving substrate accessibility for microorganisms. Hybrid methods that combine multiple techniques, such as microwave with acidic hydrolysis,[29] ultrasonic with enzymatic,[30] or heat treatment with alkaline,[31] provide improved synergies, leading to higher biogas yield and process efficiency.

Cavitation pretreatment facilitates the disintegration and solubilization of organic molecules into smaller particles, enhancing their bioavailability to biogas-producing microorganisms. Various methods, such as ultrasonication of sludge,[32] HC of ternary waste,[19] and cavitation-based processing of biomass,[33] have been employed to enhance methane and biohydrogen production. For example, treating ternary waste effluent with HC (slit venturi, at 5 bar, 120 min) resulted in better biogas yield and higher COD reduction compared to untreated effluent.[19] In another study, a 45% increase in daily biogas production was observed through the pretreatment of primary sewage sludge using ultrasonication.[34] These pretreatment methods enhance anaerobic digestion by breaking down complex organics and microbial cell walls, improving hydrolysis and substrate availability, which leads to higher methane yields and process efficiency.[35]

Sonication of DWW aids in dissociating protein aggregates, increasing solubility, and promoting the denaturation of whey proteins. It also reduces the size of lipid droplets, increasing their surface area and allowing for more microbial contact, thereby enhancing biodegradation efficiency and increasing biogas production.[19,36] In some studies, hybrid techniques, such as phase-separated sludge pretreatment using mild sonication followed by thermo-Fenton disintegration, significantly increased biogas generation. The processed sludge produced 0.187 L g^{-1} COD of biogas, demonstrating the effectiveness of this procedure in enhancing biogas production.[37] Enhancement in hydrogen production has also been reported by suppressing methanogenic bacteria through techniques like using inhibitors such as 2-bromoethanesulfonate (BES), raising organic acid concentrations (such as acetic and butyric acid), or maintaining acidic conditions (pH < 6). Additionally, increasing temperature above mesophilic ranges (>55 °C) can boost hydrogen-producing bacteria while suppressing methanogens.[5]

CG has been widely used as a feedstock for biohydrogen generation, as demonstrated in several studies. For example, thermophilic hydrogen production from CG reached a maximum yield of 1502.84 mL H_2 per L at a glycerol concentration of 20.33 g L^{-1}, utilizing *Thermoanaerobacterium* sp. bacteria.[38] In another study, biohydrogen production using both photo and dark fermentation processes with CG as a waste substrate derived from used cooking oil produced 24.06 mmol H_2 per g COD consumed in dark fermentation and 3.94 mmol H_2 per g COD consumed in photo fermentation.[39]

This study reports the production of biofuels from DWW and CG. DWW was treated using sonication and HC to enhance methane production. Additionally, DWW was mixed with CG in specific v/v ratios to increase the amount of biohydrogen generated.

2 Materials and methods

2.1 Materials

All the chemicals used in this study were purchased from Thermo Scientific India, are of analytical grade (AR), and were used as received without any further purification. The chemicals used in COD analysis were sulfuric acid (H_2SO_4), silver sulphate (Ag_2SO_4), mercuric sulphate ($HgSO_4$), potassium dichromate ($K_2Cr_2O_7$). Demineralised water was used throughout the experiment.

2.2 Compositions of CG and DWW

This study uses CG from the biodiesel industry without any pretreatment or nutrient supplementation alongside wastewater from the dairy industry. The CG, sourced from Agarwal green energy Private Ltd Jaipur, India, was stored in dark polyethylene bottles at 4 °C in the laboratory until required. The composition details of CG are provided in Table 1. The density of CG was 1.23 g mL^{-1}, and the ash content was 8.9%. This composition can vary depending on the type of catalyst used in biodiesel production and any subsequent purification processes undertaken to recover the catalyst.[40] The sample contained 7.83% sodium chloride (NaCl), likely originating from the biodiesel production process, and 2.71% matter organic non-

Table 1 Compositions of CG used in this study[a]

Parameters	CG composition & properties
pH (1% solution)	4.6
Glycerol	83.37%
Ash content	8.29%
Density	1.23 g mL^{-1}
Moisture	8.97%
Salt (NaCl)	7.83%
Non-glycerol (MONG)	2.71%
Colour	Dark brown

[a] MONG-matter organic non glycerol.

Open Access Article. Published on 12 August 2025. Downloaded on 1/21/2026 11:52:35 PM.
This article is licensed under a Creative Commons Attribution-NonCommercial 3.0 Unported Licence.

glycerol (MONG), which may include residual fats, soaps, or other organic compounds. The dark brown colour is typical of CG and reflects the presence of impurities and degradation products.

The DWW was collected from a nearby dairy farm store in Jaipur, India. Major sources of wastewater in dairy operations include waste generated during the cleaning of pipelines, transport tanks, and containers, as well as spillage from milk handling, whey processing, and sanitizing storage tanks. The DWW was stored at 4 °C in airtight, high-density polyethylene (HDPE) containers to inhibit microbial proliferation and minimize physicochemical alterations prior to experimental use. The composition of DWW is provided in Table 2. It has a pH of 7.68, with a high chemical oxygen demand (COD) of 4950 mg L^{-1} and a biological oxygen demand (BOD) of 1120 mg L^{-1}, indicating a significant organic load. The total suspended solids (TSS) content is 1230 mg L^{-1}. Additionally, the wastewater contains 6.6 mg L^{-1} of ammonium, 6.2 mg L^{-1} of ammonia, and 18.2 mg L^{-1} of phosphate. The oil and grease content are 92 mg L^{-1}, reflecting the high nutrient and organic matter levels present.

2.3 Analytical methods and data analysis

The composition of methane and hydrogen was determined using gas chromatography (GC, Thermo Scientific Trace 110) equipped with a thermal conductivity detector (TCD) and a Porapak Q column with an 80/100 mesh size, 8-inch length, and 1/8-inch diameter. The following parameters are used to operate the GC: injector temperature of 100 °C, oven temperature first maintained at 50 °C for 5 minutes, ramped up to 80 °C at a rate of 10 °C min^{-1}, and held for 5 minutes, while the detector is kept at 110 °C. Nitrogen is employed as the carrier gas at a constant flow rate of 30 mL min^{-1}. Standard gas mixtures are used for calibration, and the peak regions of the samples are compared to the standards to determine the methane and hydrogen concentrations.

VFAs are measured by taking a 1 mL sample from the anaerobic digester batch at regular intervals to determine which fatty acids are produced during anaerobic digestion and their respective concentrations. The concentration of VFAs was determined using high-performance liquid chromatography (HPLC) equipped with an AMINEX HPX-87H column (300 mm × 7.8 mm). Fatty acid concentrations were measured using a photodiode array (PDA) detector at a wavelength of 210 nm. The mobile phase used was 5 mM H_2SO_4 with a flow rate of 0.6 mL min^{-1}. The sample was filtered using a 0.45 μm (Ultipor N66 Nylon 6,6 membrane) syringe filter before injecting it into HPLC as reported in our previous work.[8,41]

The volumetric biogas production was measured using the manometric method, where pressure readings were converted into biogas volume using the ideal gas law under specific experimental conditions. Subsequently, the biogas production at standard temperature and pressure (STP: 273 K and 1 atm) was calculated. The biogas generation potential was determined using eqn (1), ensuring accuracy in production estimates. To calculate the volumetric hydrogen production, the total biogas volume was multiplied by the hydrogen content, which was determined through gas chromatography analysis.[21,42] This method provides precise quantification of hydrogen production in biogas under standardised conditions.

$$V = \frac{P \times V_h \times C}{R \times T} \times 1000 \quad (1)$$

where, V is volume of the biogas (mL), P is internal pressure of the biogas inside the bottle (mbar), V_h is available head space inside the bottle (L), C is molar volume 22.41 L mol^{-1}, R is universal gas constant, 83.14 L mbar mol^{-1} K^{-1}, T is temperature (K).

Fourier Transform Infrared Spectroscopy (FTIR) was performed on pure glycerol (PG) and CG using a PerkinElmer spectrophotometer (USA). Both samples were scanned in transmission mode over the 400 to 4000 cm^{-1} range.

The chemical oxygen demand (COD) of DWW was measured before and after treatment (US and HC), as well as after anaerobic digestion. The COD value of DWW was carried out as per the standard APHA methods (1998).[43]

2.4 DWW pretreatment using US

The collected DWW was subjected to treatment using a probe-type ultrasonic processor (VCX750, 20 kHz, Sonics & Materials, USA) under varying power amplitude and time conditions. Ultrasonic treatment was conducted at three different power amplitude levels; 30, 40 and 60%. The corresponding power supplied at these amplitudes were 225 W, 300 W and 450 W, respectively. Sonication time was varied from 15 to 60 minutes at defined intervals to study the effect of exposure duration. After sonication, the batches were prepared under the same conditions as described earlier. The US setup is shown in Fig. 1.

2.5 DWW pretreatment using HC

DWW was also treated using HC, employing a circular venturi device with a 2 mm diameter hole. The details of the device and the HC reactor system are given in Fig. 2. The experiments were conducted at different inlet pressure in the range of 3 to 7 bar(g). At each pressure, the DWW was treated for 30, 60, and 90 min and subsequently used for anaerobic digestion. After treatment with HC, the batches were prepared in the same manner as described in the previous sections.

Table 2 Compositions of DWW

Parameters	DWW composition
pH	7.68
COD	4950 mg L^{-1}
Total Suspended Solids	1230 mg L^{-1}
$NH4^+$	6.6 mg L^{-1}
NH_3	6.2 mg L^{-1}
NH_3–N	5.1 mg L^{-1}
P	6 mg L^{-1}
P_2O_5	13.6 mg L^{-1}
$(PO_4)^{3-}$	18.2 mg L^{-1}
Oil & grease	92 mg L^{-1}

 © 2025 The Author(s). Published by the Royal Society of Chemistry

Open Access Article. Published on 12 August 2025. Downloaded on 1/21/2026 11:52:35 PM.
This article is licensed under a Creative Commons Attribution-NonCommercial 3.0 Unported Licence.

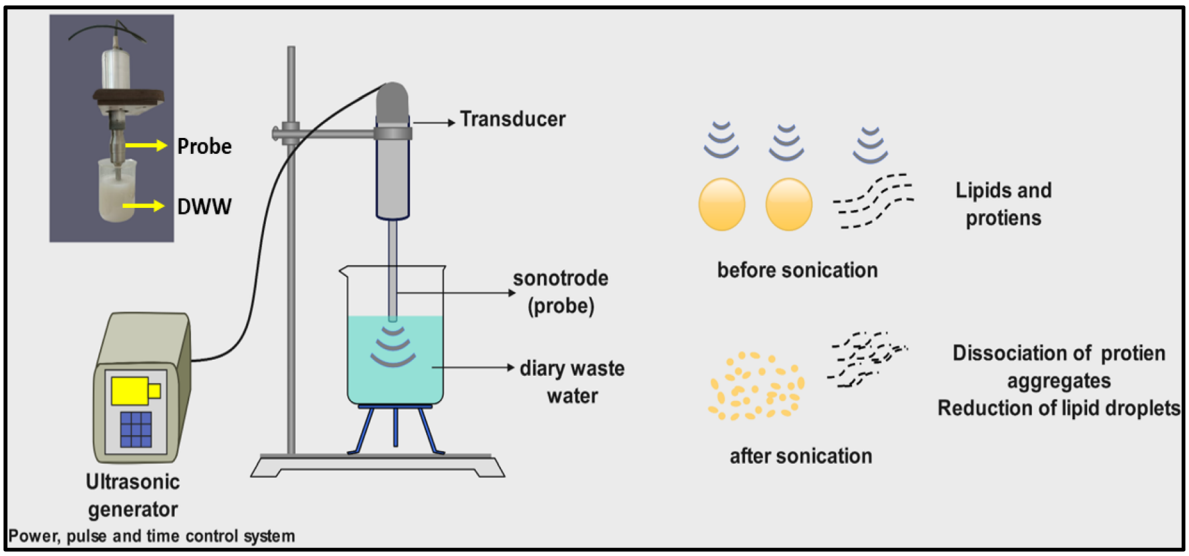

Fig. 1 US assisted pretreatment of DWW.

2.6 Mono-digestion of DWW and co-digestion of DWW with CG

The pretreated DWW, using US and HC, was subjected to anaerobic digestion in glass bottles. Separate digestion batches were conducted using DWW pretreated with US at varying power amplitudes and durations, as well as with HC at different inlet pressures. Each glass bottle had a total volume of 610 mL, with a working volume of 400 mL, leaving 210 mL of headspace for biogas accumulation. All the glass bottles were cleaned carefully and dried in the hot air oven before starting the batch experiment. 350 mL of DWW and 50 mL of inoculum were added to each bottle, which was then purged with nitrogen to establish proper anaerobic conditions. The bottles were sealed with a rubber septum and incubated at 35 °C ± 0.1 °C. Further co-digestion batches were carried out by adding different concentrations of crude glycerol (v/v%) to both untreated and

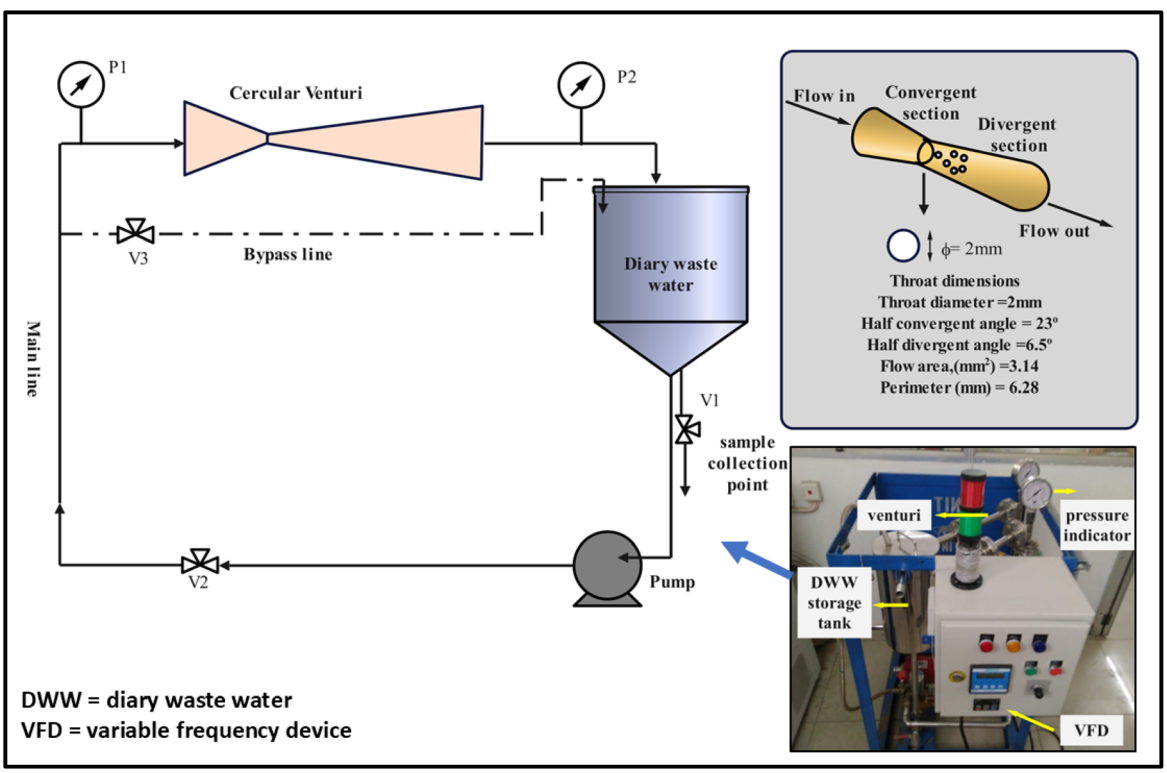

Fig. 2 HC set up and its schematic diagram along with circular venturi insight.

Open Access Article. Published on 12 August 2025. Downloaded on 1/21/2026 11:52:35 PM.
This article is licensed under a Creative Commons Attribution-NonCommercial 3.0 Unported Licence.

pretreated DWW to observe its effect on hydrogen and methane production. CG and DWW volume varied from 0.2 to 15% v/v of DWW. The amount of inoculum was 50 mL in every batch and DWW was 350 mL respectively. All these anaerobic digestion experiments were conducted in duplicate, and the results are reported as average values.

2.7 Kinetics of methane and hydrogen production

Various kinetic models are available to study methane and hydrogen production, including the first-order kinetic model, modified Gompertz model, Chen and Hashimoto model, transfer model, cone model, superimposed model, modified Gompertz combined with second-order equations, and two-phase exponential model. The modified Gompertz model offers several advantages: it provides biologically meaningful parameters such as the maximum cumulative methane/hydrogen yield, maximum production rate, and lag phase duration. Additionally, it effectively models the sigmoidal nature of biogas production curves by capturing the lag phase, exponential growth, and stationary phases.[7,44,45] In our study, we selected the modified Gompertz model because our methane and hydrogen production data exhibit a sigmoidal pattern, and this model offers multiple predicted parameters that comprehensively describe the biogas generation process. The modified Gompertz equation is stated as follows:

$$P(t) = P_{\max}\exp\left\{-\exp\left[\frac{r_m e}{P_{\max}}(\lambda - t) + 1\right]\right\} \quad (2)$$

The cumulative methane/hydrogen yield (mL) at time t is represented by $P(t)$, the maximum methane/hydrogen production rate (mL per day) by r_m, the maximum cumulative methane/hydrogen yield (mL) by $P_{\max}$, the lag phase time (day) by λ, the incubation period (day) by t, and the base of natural logarithms, e, is 2.718. The data was fitted to eqn (2) using MATLAB R2024b (academic version).

2.8 Statistical analysis

The statistical analysis was performed using response surface methodology (RSM) to study the effects of independent variables such as power amplitude, pressure, and treatment time associated with ultrasound (US) and hydrodynamic cavitation (HC) and their interactions on biogas yield. The RSM and Analysis of Variance (ANOVA) were conducted in Minitab (trial version). The statistical significance of the model and individual parameters was assessed using Fisher's F-test and probability values (p-values) to identify the most influential factors and their interactions contributing to variations in biogas production.

3 Results and discussion

3.1 FTIR analysis of PG and CG

FTIR analysis of CG and PG was conducted using an FT-IR spectrum 2 instrument (PerkinElmer, USA) over the range of 4000–400 cm^{-1} to identify the different functional groups present in the CG. The O–H stretching frequency was observed at 3293 cm^{-1} in PG and at 3306.3 cm^{-1} in CG as shown in Fig. 3. The strong peak at 1712 cm^{-1} in CG and at 1739.45 cm^{-1} in PG indicates the presence of C=O bonds, attributed to esters. In CG, this is associated with the COO group, which is related to soap impurities and is absent in the spectrum of PG.[46,47] The peak at 1032.79 cm^{-1} in CG and 1030.26 cm^{-1} in PG corresponds to the presence of primary alcohol groups (R-CH$_2$OH).[48]

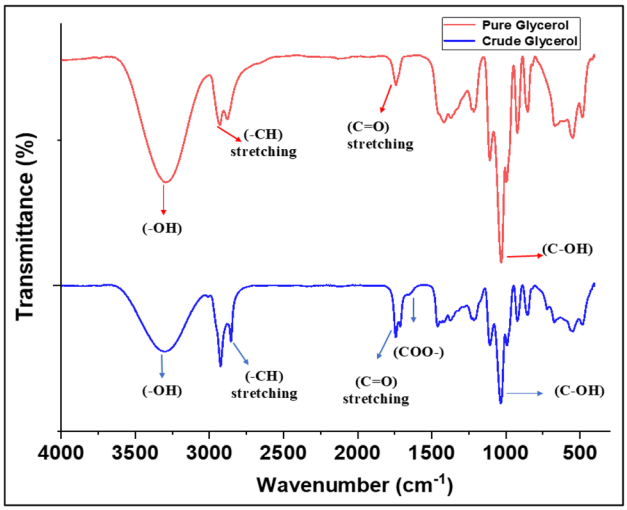

Fig. 3 FTIR of PG and CG.

3.2 Anaerobic digestion of US treated DWW

To enhance methane production through anaerobic digestion, the impact of US on DWW was studied by varying the power amplitudes and time intervals. The production of methane from untreated DWW was also performed by adding only the inoculum. The study of methane generation at different sonication conditions revealed a direct relationship between biogas yield and the process variables, such as amplitude and treatment time as shown in Fig. 4. The modified Gompertz equation was used to calculate the parameters λ, r_m, $P_{\max}$, and $P(t)$, and the results are presented in Table 3. The maximum methane yield was observed after 30 min at 60% amplitude, indicating these as the optimal conditions. At 60% amplitude and after 30 min, $P_{\max}$ was 413 mL, while $P(t)$ was 426.8 mL, with an r_m of 26.31 mL per day and a λ of 23.19 days as shown in Fig. 4. This suggests that under these conditions, the microbial consortia responsible for methanogenesis are operating at their most efficient state, likely due to improved hydrolysis and fermentation kinetics. The untreated DWW exhibited a $P_{\max}$ of 264 mL and r_m of 10.27 mL per day. The λ was prolonged to 36.49 days, indicating a delay in microbial adaptation, likely due to the complex organic content of the DWW. The r_m reached 10.27 mL per day reflecting moderate activity post-acclimation. These findings highlight the biodegradability of DWW, though the digestion process remains kinetically limited. Implementing US as a pretreatment method enhanced methane production by reducing lag time and boosting conversion rates. The rate (r_m) consistently increases with amplitude, implying that higher

 © 2025 The Author(s). Published by the Royal Society of Chemistry

Open Access Article. Published on 12 August 2025. Downloaded on 1/21/2026 11:52:35 PM.
This article is licensed under a Creative Commons Attribution-NonCommercial 3.0 Unported Licence.

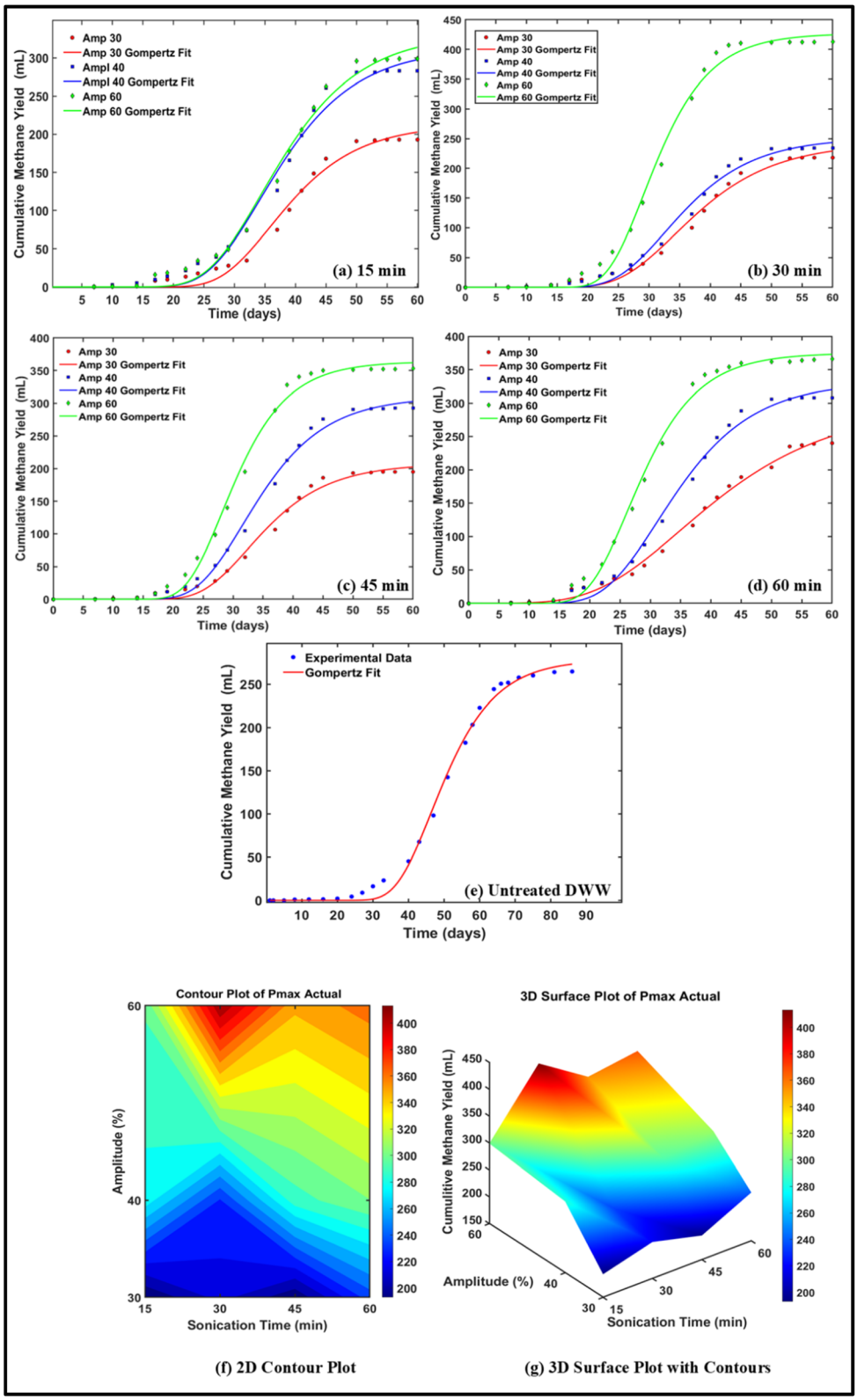

Fig. 4 Effect of sonication duration and amplitude on methane generation from DWW: (a) 15 min at amplitude of 30, 40, and 60; (b) 30 min at amplitude of 30, 40, and 60; (c) 45 min at amplitude of 30, 40, and 60; (d) 60 min at amplitude30, 40 and 60. (e) Untreated DWW (f) 2 D Contour Plot, and (g) 3D surface plot with contour for anaerobic digestion of ultrasonicated DWW.

ultrasound intensities improve microbial activity and substrate disintegration, as shown in Table 3. However, at longer sonication times, 60 min, r_m shows a slight decline at 60% amplitude with the rate of 21.42 mL CH_4 per day, suggesting that prolonged sonication may begin to disrupt microbial integrity or lead to excessive substrate breakdown and the

Open Access Article. Published on 12 August 2025. Downloaded on 1/21/2026 11:52:35 PM.
This article is licensed under a Creative Commons Attribution-NonCommercial 3.0 Unported Licence.

Table 3 Modified Gompertz parameters for anaerobic digestion of ultrasonicated DWW

Sonication time	Amplitude	P_{max} actual (mL)	$P(t)$ Gompertz (mL)	R^2	r_m (mL per day)	λ (days)
15	30	193	213.1	0.9875	9.7	27.81
	40	283	313.13	0.9884	13.33	25.60
	60	299	332.02	0.9904	13.73	25.56
30	30	218	242.66	0.9906	9.91	25.27
	40	234	251.48	0.9922	11.6	24.64
	60	413	426.8	0.9942	26.31	23.19
45	30	195	207.46	0.9917	10.22	24.93
	40	293	309.99	0.9956	15.06	24.04
	60	353	363.7	0.9949	22.36	22.22
60	30	240	296.54	0.9943	7.76	20.90
	40	308	332.08	0.9942	14.018	22.43
	60	366	374.84	0.9956	21.42	19.78
Untreated DWW	—	264	278.34	0.9961	10.27	36.49

degradation, limiting further methane production. The value λ decreases with increasing amplitude and sonication time. The shortest λ (19.78 days) was observed after 60 minutes at 60% amplitude, suggesting that intense ultrasound treatment accelerates microbial acclimatization and enhances substrate bioavailability. The longest λ of 27.8 days was observed at 30% amplitude and sonication time of 30 min. However, prolonged exposure beyond 30 min does not significantly enhance r_m or P_{max}, indicating that an optimal sonication duration exists beyond which process efficiency does not improve due to degradation of substrate. Fig. 4(f) and (g) demonstrate that P_{max} generally increases with both sonication time and amplitude. Notably, substantial P_{max} values (ranging from 234 to 413 mL) were achieved with moderate sonication time durations of 30–45 min combined with higher amplitudes (40–60%), suggesting an optimal range for efficient gas production. In contrast, all time intervals produced lower P_{max} values at the lowest amplitude setting (30%), indicating that limited energy input constrains conversion efficiency.

This trend can be attributed to enhanced cavitation and turbulence at higher amplitudes, which promote greater cell disruption, increased enzymatic hydrolysis, and improved substrate bioavailability for microbial metabolism. These results highlight the fact that increasing amplitude and sonication time can improve methane yield and production rate, however there is a threshold beyond which excessive ultrasound might result in decreasing return. The plateauing of methane production and the decline in r_m with longer sonication periods is possibly due to substrate degradation, severe cell damage, or microbial weariness. When the results of untreated DWW were compared with those of pretreated DWW using US, a significant improvement was observed in both P_{max} and r_m. These values were considerably higher for the pretreated DWW subjected to anaerobic digestion compared to the untreated DWW. US pretreatment enhances anaerobic digestion by breaking down bio-recalcitrant compounds into smaller, more biodegradable molecules. This is primarily achieved through the generation of hydroxyl radicals ($^{\bullet}OH$), which help disintegrate complex organic molecules. Additionally, the pressure shock waves produced during US aid in breaking larger solid particles, increasing their solubility and making them more accessible to microbial degradation. Overall, the study clearly demonstrates that US assisted pretreatment leads to enhanced methane production, improved production rates, and a shorter lag phase during anaerobic digestion.

The most important element for increasing P_{max} and r_m is amplitude, whereas sonication time mainly lowers the lag phase. But after 30 min, the advantages of prolonged sonication fade. For the highest methane yield and production rate while preserving microbial viability, 30 min of sonication at 60% amplitude provides the ideal conditions for maximum efficiency. Sonication not only enhanced the P_{max} but also significantly reduced the lag phase duration, leading to an improved r_m when compared to untreated DWW.

Response Surface Methodology (RSM) was employed to statistically analyze the influence of process parameters on methane yield (P_{max}), focusing on both individual and interactive effects under ultrasonic conditions. The analysis revealed a significant dependency of methane yield on ultrasonic parameters. Analysis of Variance (ANOVA) indicated that power amplitude had a more pronounced effect than sonication time, as evidenced by a higher F-value (30.09; $p < 0.05$). A clear linear relationship between amplitude and methane yield was observed, suggesting that the individual impact of amplitude was greater than that of time or any interactive effects.

3.3 Anaerobic digestion of HC treated DWW

The effect of HC on methane production has been investigated using a venturi device with a hole size of 2 mm, and its configuration details are provided in Fig. 2. The DWW was pretreated using HC at various pressures ranging from 3 to 7 bar, with treatment durations of 30, 60, and 90 minutes at each pressure. The pretreated DWW was subjected to anaerobic digestion following the procedure outlined in Section 2.4. The cumulative methane yield under these conditions is shown in Fig. 5. The experimental data were fitted using the modified Gompertz equation (eqn (2)), and the corresponding Gompertz parameters are presented in Table 4. The cumulative methane

 © 2025 The Author(s). Published by the Royal Society of Chemistry

Open Access Article. Published on 12 August 2025. Downloaded on 1/21/2026 11:52:35 PM.
This article is licensed under a Creative Commons Attribution-NonCommercial 3.0 Unported Licence.

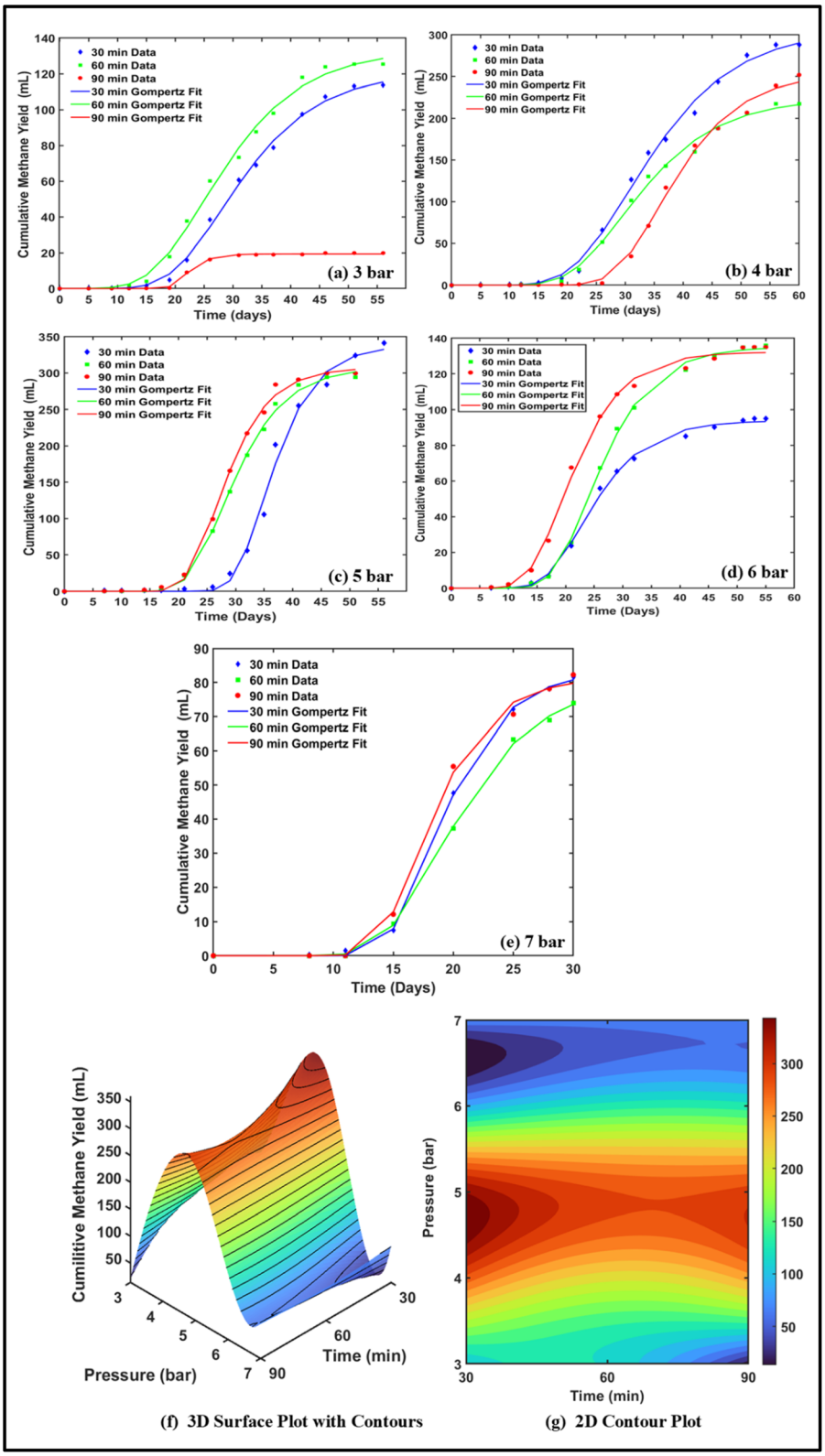

Fig. 5 Cumulative Methane yield from DWW treated by HC at different pressures: (a) 3 bar, (b) 4 bar, (c) 5 bar, (d) 6 bar, and (e) 7 bar. (f) 3D surface plot and (g) 2D contour plot.

yield from HC treated DWW at different pressures and times is also presented as 3D surface and contour plots, as shown in Fig. 5(f) and (g).

The Gompertz model, which determines the P_{max}, r_m and λ values at various cavitation pressures (3–7 bar) and treatment times (30, 60, and 90 min), was used to analyse the kinetic

Open Access Article. Published on 12 August 2025. Downloaded on 1/21/2026 11:52:35 PM.
This article is licensed under a Creative Commons Attribution-NonCommercial 3.0 Unported Licence.

Table 4 Modified Gompertz parameters for anaerobic digestion of HC treated DWW

Pressure (barg)	Time	P_{max} actual (mL)	P_{max} Gompertz (mL)	R^2	r_m	λ (days)
3	30	113.74	121.16	0.9978	4.85	18.95
	60	125.4	133.48	0.9957	5.21	15.56
	90	19.89	19.38	0.9982	3.04	19.18
4	30	287.95	306.27	0.9966	11.21	20.59
	60	217.32	224.51	0.9968	9.03	20.37
	90	251.9	254.5	0.9967	12.03	28.03
5	30	341.21	337.84	0.9930	24.43	29.74
	60	294.28	308.31	0.9986	18.67	21.56
	90	299.67	307.60	0.9983	21.91	21.33
6	30	95.07	93.97	0.997	5.46	16.34
	60	136.01	135.17	0.9989	7.90	17.60
	90	135.8	132.27	0.9969	8.18	13.37
7	30	81.64	83.48	0.9996	8.74	14.51
	60	74.1	80.37	0.995	6.34	14.01
	90	82.25	81.49	0.9978	8.94	13.70

behaviour of methane production under HC. The robust fit of the model to the experimental data is confirmed by the high R^2 values (>0.99), which show a clear correlation between the kinetics of methane production and cavitation conditions.

As pressure increases, methane yield increases with pressure and time, reaching a peak at 5 bar and 30 min, then decreases, indicating enhanced microbial activity at optimal conditions and inhibition at higher pressures. Pressure and treatment duration have a substantial impact on the potential for methane generation. At 5 bar and 30 min, the P_{max} value of 341.21 mL was recorded, indicating that this condition provides optimal cavitation energy to enhance microbial activity without causing excessive cell damage. When compared with the results of untreated DWW, which exhibited a P_{max} of 264 mL and a prolonged λ of 36.49 days, as shown in Fig. 4(e), it is evident that pretreatment using HC significantly enhanced methane yield and production rate while reducing the lag phase. From Table 4, it can be seen that the methane generation either decreases or remain constant after a critical treatment time at a given pressure. At a given time, when the pressure was increased from 3 to 5 bar, methane generation (P_{max}) increased, but it significantly decreased when the pressure was further raised to 7 bar. The decrease in the methane yield was attributed to over-processing effects induced by excessive cavitational treatment, which led to the degradation of substrate molecules. This degradation likely interferes with microbial metabolism during anaerobic digestion, thereby reducing the overall biogas yield.

Further, the statistical analysis of the obtained data was performed using RSM to understand individual and interactive effects of process parameters on methane yield (P_{max}). It was observed that the individual effects of pressure and treatment time were statistically insignificant ($p > 0.05$), with no evident linear relationship between these parameters and methane yield. However, the quadratic effect of pressure was found to be statistically significant, as reflected by a higher F-value (22.55; $p < 0.05$), suggesting a non-linear influence on the yield (P_{max}). These findings are likely attributable to over-processing effects that occur beyond a critical cavitational threshold, leading to diminished methane production after 5 bar.

The r_m follows a similar trend as P_{max}, with the highest value obtained at 5 bar and 30 min (24.43 mL per day), indicating rapid methane production once the λ is overcome. However, at the same pressure, on extending the treatment time to 60 and 90 min, r_m was reduced (18.67 and 21.91 mL per day, respectively), suggesting that prolonged cavitation does not enhance methane production kinetics. At 6 and 7 bar, r_m declines further, with the lowest observed value at 7 bar and 60 min (80.37 mL), implying microbial inhibition due to substrate degradation. The λ represents the adaptation period before methane production reaches its exponential phase. The longest lag phase was observed at 5 bar and 30 min (29.74 days), suggesting that although microbial adaptation takes longer, the methane yield is ultimately maximized. In contrast, at 7 bar and 60 min, λ was 14.01 days, but methane yield is minimal, indicating that extreme cavitation degrades substrate, thereby reducing microbial activity before significant methane production can occur. At 6 and 7 bar, methane production declines significantly. At 6 bar, the highest methane yield is observed at 60 min (136.01 mL CH_4, $r_m = 7.90$ mL per day), but at 90 min, methane yield stagnates at 135.80 mL CH_4, indicating a plateau in the microbial response to cavitation. At 7 bar, the lowest methane production occurs at 60 min (only 74.1 mL CH_4, $r_m = 6.34$ mL per day), with marginal recovery at 90 min (82.25 mL CH_4, $r_m = 8.94$ mL per day). The decreasing trend at these higher pressures suggests that excessive cavitation forces might disrupt microbial cells, strip dissolved gases, or lead to excessive radical formation that degrades the organic substrates necessary for methanogenesis. In HC, $^{\bullet}OH$ radicals are generated, which aid in breaking down large, bio-recalcitrant molecules into smaller, more biodegradable compounds. The primary objective of using HC in this study was to enhance methane yield by pre-treating DWW before subjecting it to anaerobic digestion. The results indicate that HC effectively increases methane yield up to a certain inlet pressure, specifically, 5 bar. As the inlet pressure to the cavitating device increases, the cavitation number decreases, which promotes the generation of more hydroxyl radicals. This enhanced radical production at moderate pressures (from 3 to 5 bar) improves the

 © 2025 The Author(s). Published by the Royal Society of Chemistry

Open Access Article. Published on 12 August 2025. Downloaded on 1/21/2026 11:52:35 PM. This article is licensed under a Creative Commons Attribution-NonCommercial 3.0 Unported Licence.

breakdown of complex molecules, resulting in a higher availability of biodegradable substrates for anaerobic digestion and, consequently, increased methane yield.

However, when the inlet pressure exceeds 5 bar, the excessive generation of ˙OH radicals begin to degrade not only the complex molecules but also the intermediate compounds that serve as substrates for microorganisms. As a result, fewer substrates are available for microbial activity during anaerobic digestion, leading to a decline in methane production. Therefore, HC pretreatment should be conducted at moderate pressures. Higher inlet pressures may lead to excessive degradation of organic matter, ultimately reducing the efficiency of methane generation.

Overall, the kinetic trends suggest that 5 bar and 30 min is the optimal condition for methane production, yielding the highest P_{max} (341.21 mL CH_4), the highest r_m (24.43 mL per day), and an extended λ (29.74 day), indicating a delayed but highly efficient methane generation process. In contrast, higher pressures (6 to 7 bar) resulted in a decline in methane yield and lower methane production rates, despite shorter lag phases. Extended treatment times beyond 30 min show mixed effects, with 60–90 min at 5 bar slightly reducing P_{max} and r_m, suggesting diminishing returns. Moreover, when compared to untreated DWW, HC with optimum parameters significantly enhanced P_{max}, reduced lag phase duration, and improved methane r_m, as shown in Fig. 5(f), (g) and 4(e).

The high R^2 values (>0.99) confirm that methane production follows predictable Gompertz kinetics under different cavitation conditions. These findings indicate that a pressure of 5 bar with a treatment duration of 30 min provides the best balance between microbial adaptation and methane yield, while higher pressures (6–7 bar) should be avoided as it degrades substitute leading to microbial inhibition. Extended treatment beyond 30 min offers limited benefits and may negatively impact methane yield.

3.4 Effect of US and HC on COD reduction

The data presented in Table 5 demonstrate the influence of sonication time and amplitude on the efficiency of COD removal and P_{max}, highlighting the effectiveness of ultrasound-assisted treatment for DWW. It has been observed that as the amplitude of sonication increases, the COD decreases, indicating that higher amplitudes lead to more efficient breakdown of organic matter in the wastewater. This suggests that higher amplitude helps to break down larger organic compounds into smaller, which can be easily digested by the microorganisms in the anaerobic digestion process.

In addition, the results show a clear trend where longer sonication times improve the removal of COD. With longer sonication durations, the COD after anaerobic digestion tends to be lower, reflecting a more effective pre-treatment of the wastewater. This implies that extending the sonication time further enhances the breakdown of organic material, which contributes to more efficient anaerobic digestion. Furthermore, the data shows that increasing the amplitude and duration of sonication generally results in higher methane production. For example, at higher amplitude (60%) and longer sonication times (30–60 min), methane production reaches its peak, which aligns with more significant COD removal. This indicates that both the amplitude and the duration of sonication can significantly influence the efficiency of anaerobic digestion and the subsequent methane production.

The effect of HC on COD reduction is summarized in Table 6. When DWW was treated using HC followed by anaerobic digestion, it was observed that total COD reduction increased with pressure, reaching a maximum at 5 bar. However, beyond 5 bar, COD reduction began to decline, particularly at 6 and 7 bar. Although the COD reduction was almost similar at 4 and 5 bar, the subsequent anaerobic digestion resulted in a greater COD reduction and higher methane generation at 5 bar. As the pressure increases, the cavitation number decreases, leading to the formation of a greater number of cavitation bubbles and consequently higher production of hydroxyl ˙OH radicals at pressures of 6 and 7 bar. These radicals further degrade the intermediates formed from the breakdown of bio-recalcitrant molecules, resulting in fewer biodegradable substrates available for subsequent anaerobic digestion. As a result, both methane yield and COD reduction decrease when DWW is pretreated at pressures above 5 bar. Mild cavitation at 5 bar is sufficient to break down complex molecules, while more intensive cavitation at higher pressures may excessively degrade these intermediates, reducing their biodegradability. It was also

Table 5 Summary of COD and P_{max} trends when DWW treated with US

Amplitude (%)	Sonication time (min)	COD initial (mg L^{-1})	COD after US (mg L^{-1})	COD after anaerobic digestion (mg L^{-1})	Total % COD reduction	P_{max} actual (mL)
30	15	4950	4800	950	80.81	193
	30		3980	942	80.97	218
	45		3750	640	87.07	195
	60		3735	610	87.68	240
40	15		4520	720	85.45	283
	30		4070	567	88.55	234
	45		3970	380	92.32	293
	60		3930	320	93.54	308
60	15		4800	688	86.10	299
	30		4160	530	89.29	413
	45		4030	430	91.31	353
	60		4050	320	93.54	366

Open Access Article. Published on 12 August 2025. Downloaded on 1/21/2026 11:52:35 PM.
This article is licensed under a Creative Commons Attribution-NonCommercial 3.0 Unported Licence.

Table 6 Summary of COD reduction and P_{max} trends for DWW treated with HC

Pressure (barg)	Time (min)	COD initial (mg L^{-1})	COD after HC (mg L^{-1})	COD after anaerobic digestion (mg L^{-1})	Total % COD reduction	P_{max} actual (mL)
3	30	4950	3253	295	94.04	113.74
	60		2434	140	97.17	125.4
	90		2419	159	96.79	19.89
4	30		3960	90	98.18	287.95
	60		2550	82	98.34	217.32
	90		2380	83	98.32	251.9
5	30		3370	80	98.38	341.21
	60		3170	29	99.41	294.28
	90		2310	31	99.37	299.67
6	30		3050	270	94.55	95.07
	60		2590	182	96.32	136.01
	90		2330	170	96.57	135.8
7	30		3200	220	95.56	81.64
	60		3130	162	96.73	74.1
	90		2830	108	97.82	82.25

observed that increasing the treatment time at all pressure levels led to greater COD reduction during HC. However, when this pretreated DWW was subjected to anaerobic digestion, the COD reduction did not significantly improve beyond 30 minutes of cavitation treatment. This suggests that 30 minutes of HC is sufficient to break down larger organic molecules into smaller ones, which can then be more easily digested by microorganisms during anaerobic digestion.

In conclusion, both US and HC serve as effective pretreatment methods for enhancing anaerobic digestion of DWW.

3.5 Co-digestion of DWW with CG for hydrogen production

CG is a highly fermentable substrate that acts as an effective carbon source and raises the general metabolic activity of the microbial communities that participate in anaerobic digestion. Its inclusion can increase microbial activity and propels the system toward hydrogen generation by stimulating microorganisms that produce hydrogen. By favouring acidogenic fermentation pathways over methanogenesis, glycerol creates an environment conducive to hydrogen synthesis. Additionally, it inhibits methanogens from producing methane, thereby redirecting electron flow towards increased hydrogen production.[38,49,50]

Co-digestion of DWW was carried out at different CG concentration, varied from 0.2 to 15% v/v and the results are shown in Fig. 6 and 7. At lower glycerol concentrations (0.2–0.6% v/v), methane production is the dominant pathway, with the highest yield observed at 0.2% CG (P_{max} = 59.19 mL) as shown in Fig. 6(a). This condition is associated with a significant λ (24.65 days), indicating a slow establishment of methanogenic microbial activity, as shown in Table 7. The high correlation coefficient (R^2 = 0.9969) suggests that methane production follows a well-defined kinetic trend. However, with increasing glycerol concentration, methane yield declines sharply, falling to just 0.958 mL at 1% CG and accompanied by a lower r_m of 0.035 mL per day as shown in Table 7. This suggests that higher glycerol concentrations lead to the excessive accumulation of metabolic intermediates such as VFAs and alcohols, which can inhibit methanogenesis and disrupt the balance of microbial consortia, ultimately impairing the efficiency of anaerobic bioconversion. Studies have shown that using CG alone or in high concentrations during anaerobic digestion can suppress the activity of methane-producing microorganisms, resulting in reduced biogas and methane output. This highlights the importance of optimizing glycerol dosing to avoid inhibitory effects while maintaining a stable and efficient microbial environment for bioenergy production.[50,51]

In contrast, hydrogen production exhibits an increasing trend at moderate glycerol concentrations from 1–6%, where acidogenesis and acetogenesis are the predominant metabolic pathways as shown in Fig. 6. At 1% CG, hydrogen yield reaches 49.09 mL, with a high r_m of 4.66 mL per day and a shorter λ (1.427 days), indicating a rapid microbial response. Hydrogen production peaks at 4% CG (P_{max} = 330.8 mL), coupled with the highest observed r_m of 45.6 mL per day and a minimal λ (0.69 days), reflecting optimal substrate utilization. These findings suggest that acidogenic and acetogenic pathways efficiently convert glycerol into metabolic intermediates at these concentrations, leading to enhanced hydrogen yields. Table 7 shows the methane and hydrogen production affected by CG concentration along with Gompertz fitting data.

As shown in Fig. 7, Beyond 6% v/v CG, hydrogen yield also decline, likely due to substrate inhibition and metabolic stress. At 10% v/v CG, hydrogen yield drops sharply to 13.90 mL (P_{max}), with a reduced r_m of 2.74 mL per day and a prolonged λ (1.48 days), indicating microbial inhibition and inefficient substrate conversion. Similarly, methane production shows a substantial decline, with almost negligible amounts produced beyond 1% v/v CG, further confirming the threshold beyond which methanogenic activity is suppressed, as shown in Fig. 7. The inhibition at these concentrations highlights the need for process optimization to prevent metabolic imbalances that hinder biogas production efficiency.

 © 2025 The Author(s). Published by the Royal Society of Chemistry

Open Access Article. Published on 12 August 2025. Downloaded on 1/21/2026 11:52:35 PM.
This article is licensed under a Creative Commons Attribution-NonCommercial 3.0 Unported Licence.

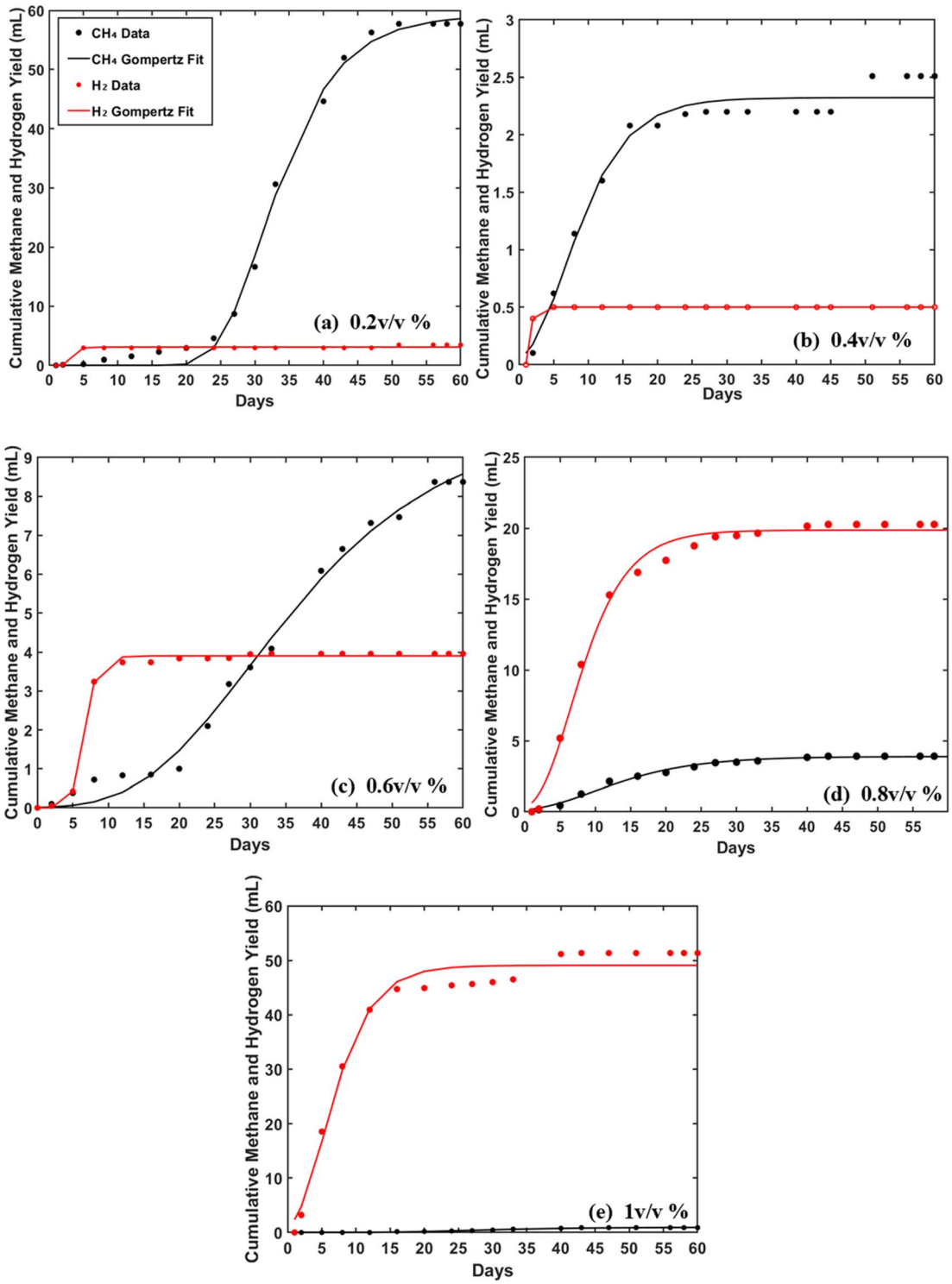

Fig. 6 Effect of glycerol addition on methane and hydrogen yield: (a) 0.2 v/v%, (b) 0.4 v/v%, (c) 0.6 v/v%, (d) 0.8 v/v%, (e) 1 v/v%.

From a kinetic perspective, the Gompertz model demonstrates excellent predictive capability, with high R^2 values (>0.98 in most cases) as shown in Table 7, reinforcing the reliability of the observed trends. The variation in lag phases across different glycerol concentrations underscores the differential adaptability of microbial populations, where methanogens exhibit slower response times compared to acidogenic and acetogenic bacteria. The transition from acidogenesis to methanogenesis is evident in the kinetic data, with hydrogen-producing pathways exhibiting shorter lag phases and higher production rates, while methane formation follows slower kinetics and is more susceptible to inhibition at elevated glycerol concentrations.

Open Access Article. Published on 12 August 2025. Downloaded on 1/21/2026 11:52:35 PM.
This article is licensed under a Creative Commons Attribution-NonCommercial 3.0 Unported Licence.

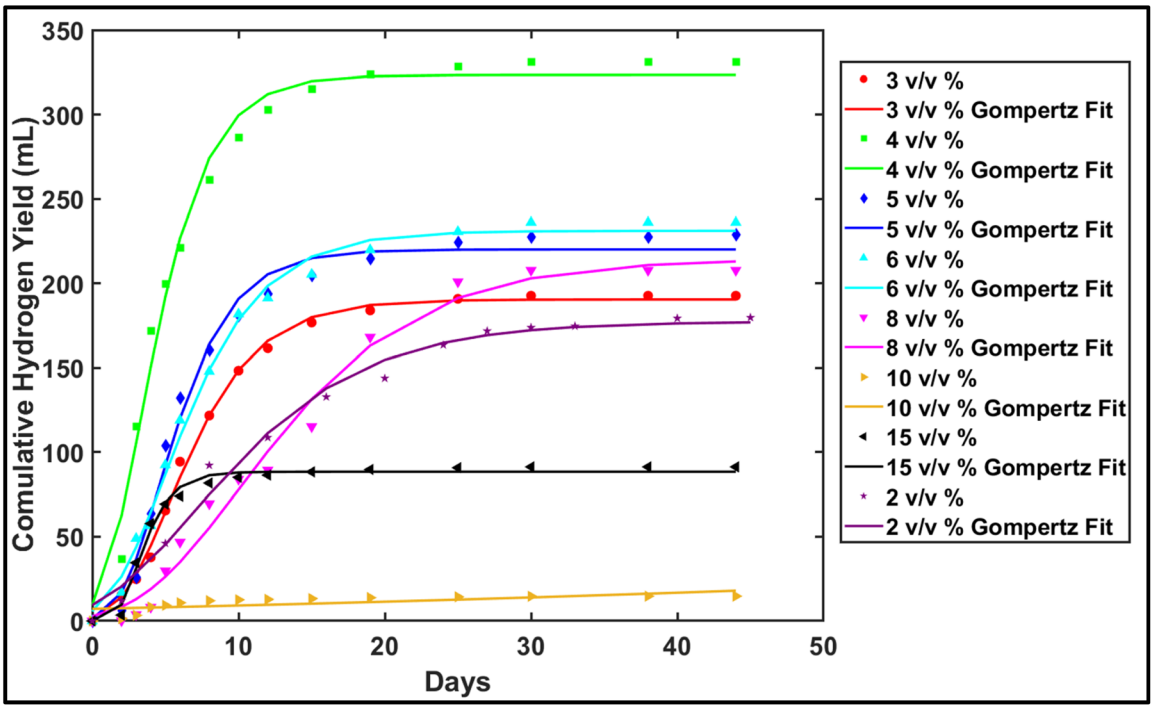

Fig. 7 Effect of glycerol addition (2% v/v to 15% v/v) on hydrogen yield.

In conclusion, glycerol concentration plays a pivotal role in determining the efficiency of hydrogen production, with distinct metabolic shifts observed at varying substrate levels. An optimal CG concentration of 4% v/v enhanced hydrogen production by maintaining a favourable balance between acidogenesis, acetogenesis, and methanogenesis. While methane production inhibits after 1% v/v CG concentration. Beyond this range, metabolic inhibition limits both pathways, necessitating process control strategies such as pH regulation, co-substrate supplementation, or adaptive microbial consortia to mitigate inhibition effects.

3.6 Volatile fatty acid formation during co-digestion of DWW with CG

The amount of volatile fatty acids (VFAs) was measured for a batch with a CG concentration of 4% v/v, combined with DWW, as this concentration comparatively produced highest hydrogen. The VFAs produced are presented in Fig. 8 and the HPLC chromatogram of the VFAs is shown in SI file (Fig. S1). As

Table 7 Modified Gompertz parameters for addition of glycerol into DWW

CG concentration (v/v%)	CH_4/H_2	$P(t)$ Gompertz (mL)	P_{max} actual (mL)	R^2	r_m (mL per day)	λ (days)
0.2	CH_4	59.19	57.75	0.9969	3.46	24.65
	H_2	3.05	3.43	0.9545	1.60	2.15
0.4	CH_4	2.32	2.51	0.9769	0.172	1.73
	H_2	0.5	0.5	1.000	0.667	1.31
0.6	CH_4	9.86	8.37	0.9932	0.236	14.55
	H_2	3.90	3.96	0.9975	1.17	4.74
0.8	CH_4	3.88	3.91	0.9912	0.180	1.87
	H_2	19.86	20.27	0.9927	1.65	2.06
1	CH_4	0.958	0.89	0.9872	0.035	15.60
	H_2	49.09	51.36	0.9792	4.66	1.427
2	H_2	177.35	179.69	0.9887	10.01	0.50
3	H_2	190.44	192.6	0.9973	20.63	1.86
4	H_2	323.41	330.8	0.9883	45.6	0.69
5	H_2	220.12	228.9	0.9894	29.28	1.85
6	H_2	231.15	236.14	0.9939	22.62	1.15
8	H_2	214.53	207.79	0.9872	11.48	3.22
10	H_2	13.90	14.72	0.9777	2.74	1.48
15	H_2	88.41	91.25	0.9887	24.56	1.72

 © 2025 The Author(s). Published by the Royal Society of Chemistry

Open Access Article. Published on 12 August 2025. Downloaded on 1/21/2026 11:52:35 PM.
This article is licensed under a Creative Commons Attribution-NonCommercial 3.0 Unported Licence.

shown in Fig. 8, VFA formation is low during the initial phase. Over the period of time, glycerol breaks into propionic acid, while the concentration of butyric acid remains relatively constant. The initial GC measurements indicated high CO_2 production. From Fig. 8, the VFA profile reflects key metabolic shifts during glycerol degradation. Initially, no VFAs are detected on Day 0, suggesting microbial adaptation. By Day 4, lactic acid (293.85 mg L^{-1}) and butyric acid (437.66 mg L^{-1}) accumulate, which is characteristic of lactic acid and butyrate fermentation pathways. At this stage, acetic acid (84.9 mg L^{-1}) and propionic acid (154.35 mg L^{-1}) suggest early acidogenesis, where glycerol is converted into VFAs and hydrogen. However, the subsequent decline in lactic acid suggests its conversion into acetic acid and hydrogen. From Day 7 onward, propionic acid increases significantly, reaching 2768.53 mg L^{-1} by Day 23, indicating that hydrogen-consuming bacteria are active, competing with hydrogen-producing pathways. Despite this, the absence of methane suggests methanogens are either inhibited or absent, likely due to low pH, short retention time, or operational conditions favouring hydrogen production. Butyric acid remains high, peaking at 800.90 mg L^{-1} on Day 11 before gradually decreasing, aligning with a typical butyrate-type fermentation that co-produces hydrogen.

By Day 32, propionic acid (3004.26 mg L^{-1}) dominates, butyric acid declines to 622.21 mg L^{-1}, and acetic acid increases to 146.29 mg L^{-1}, indicating continued VFA accumulation with no conversion into methane. The metabolic shift from butyrate to propionate production may be influenced by hydrogen partial pressure, as high hydrogen concentrations can favour propionic acid formation over butyrate. This confirms a hydrogen fermentation system, where glycerol is primarily converted into VFAs (especially PA and BA) alongside hydrogen gas instead of methane.

3.7 Co-digestion of US and HC treated DWW with CG

The maximum methane production in the US treatment, as shown in Fig. 9, was observed at the amplitude 30% and time 30 min, amplitude 40% and time 60 min, and amplitude 60% and time 30 min. Under these optimized conditions, 4% v/v CG was added to investigate its effect on hydrogen production as shown in Fig. 9(a). The same applies to the HC treatment, where maximum methane production was observed at a pressure of 5 bar and a time of 30 min as shown in Fig. 9(b). Under these conditions, 4% v/v CG was added to evaluate its impact on hydrogen production. The observed cumulative hydrogen yield is shown in the Fig. 9(a) for the US and Fig. 9(b) for the HC treatment.

At different US conditions, the highest hydrogen yield was observed at 30% amplitude and 30 min, with an actual production of 208.59 mL and a predicted value of 189.39 mL as shown in Table 8. This condition also exhibited the highest hydrogen production rate (48.0 mL per day) with a moderate λ of 2.61 days. Increasing the treatment time to 60 min resulted in a lower hydrogen yield (179.60 mL actual) and a decreased production rate (23.435 mL per day), while the λ shortened slightly to 2.12 days. Further, increasing the amplitude to 60%, led to the lowest hydrogen yield among the US conditions (136.45 mL actual) after 30 min, but with a slightly improved hydrogen production rate of 34.49 mL per day. Wherein, HC at a pressure of 5 bar for 30 min yielded 137.79 mL of hydrogen at a rate of 8.09 mL per day. However, this condition exhibited the shortest λ (0.107 days), indicating a rapid onset of hydrogen generation. However, these results show a lower yield compared

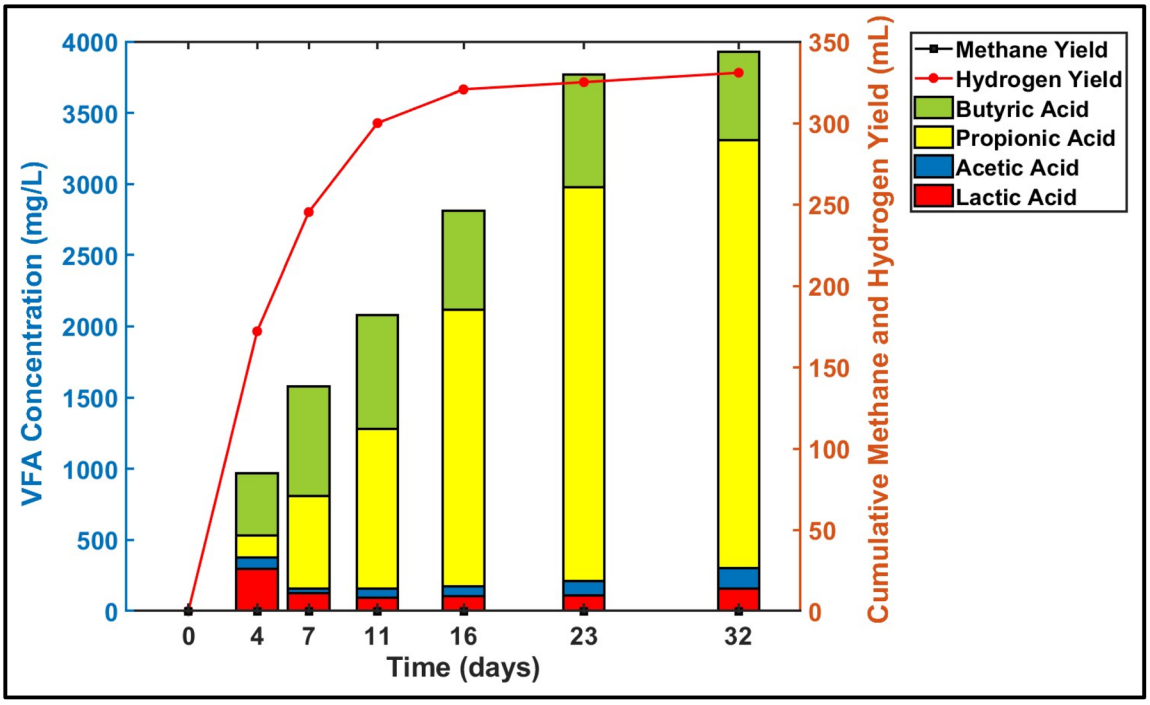

Fig. 8 Production of VFAs and hydrogen during co-digestion of DWW with CG.

Open Access Article. Published on 12 August 2025. Downloaded on 1/21/2026 11:52:35 PM.
This article is licensed under a Creative Commons Attribution-NonCommercial 3.0 Unported Licence.

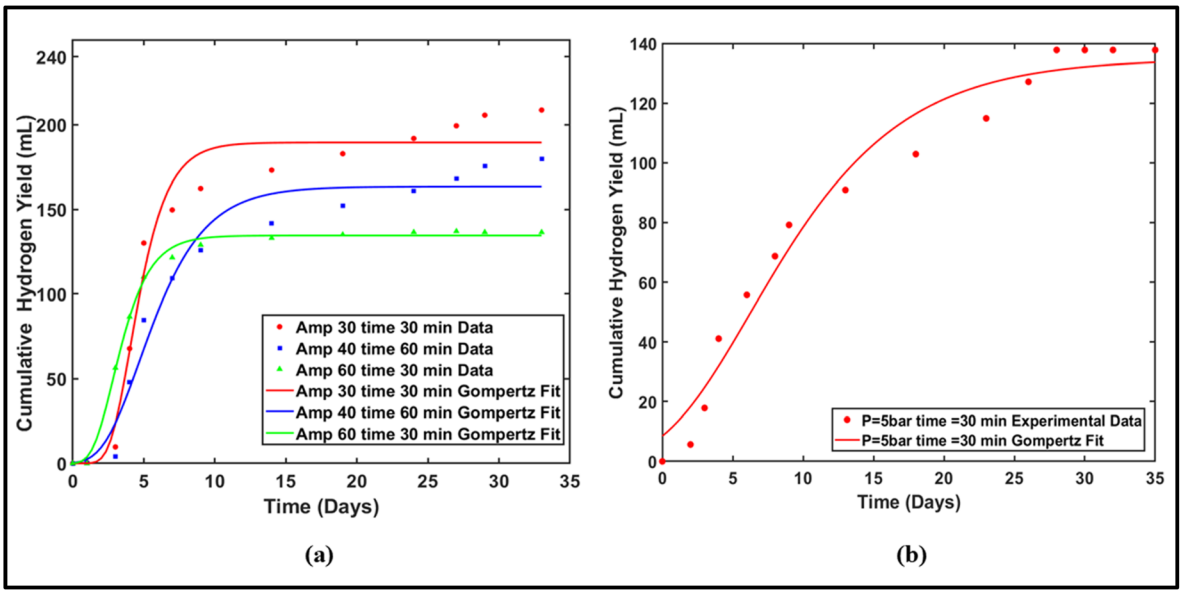

Fig. 9 (a) US treated DWW with glycerol addition; (b) HC treated DWW with glycerol addition.

Table 8 DWW treated with US and HC with addition of CG at 4 v/v%

Ultrasonication (US)/HC conditions	$P(t)$ Gompertz (mL)	P_{max} actual (mL)	R^2	r_m (mL per day)	λ (days)
30% amplitude – 30 min	189.39	208.59	0.971	48.0	2.61
40% amplitude – 60 min	163.45	179.60	0.971	23.435	2.12
60% amplitude – 30 min	134.52	136.45	0.997	34.49	1.39
HC – 5 bar – 30 min	134.91	137.79	0.971	8.09	0.107

to the co-digestion of untreated DWW with CG, suggesting that when DWW is pretreated using US and HC, hydrogen production is not enhanced compared to untreated DWW. The addition of CG to ultrasonicated and HC treated DWW resulted in a lower hydrogen yield than that achieved with untreated DWW. Therefore, it can be said that these treatment techniques (ultrasonic and HC) are only effective for methane production but not for hydrogen production.

4 Conclusions

This study highlights the significant potential of anaerobic digestion for renewable energy generation from DWW, both through standalone treatment and co-digestion with CG. Methane was produced when DWW was digested alone, and its yield was substantially enhanced by physical pretreatment methods. Specifically, US (60% amplitude, 30 min) and HC (5 bar, 30 min) improved methane production rates by increasing substrate availability and accelerating microbial activity.

In contrast, co-digestion of DWW with CG enabled the simultaneous production of methane and hydrogen, with a notable shift in metabolic pathways depending on the CG concentration. At low CG concentrations (up to 1% v/v), methane generation occurred alongside hydrogen, though at reduced levels. However, beyond 1% v/v CG, methane production was suppressed, and hydrogen became the dominant product, indicating a metabolic shift toward acidogenesis and acetogenesis. The optimal hydrogen yield was achieved at 4% v/v of CG, with a peak production rate of 45.69 mL per day and a minimal λ (0.69 days).

These findings demonstrate that methane production from DWW can be significantly enhanced *via* pretreatment, while co-digestion with CG enables a shift toward hydrogen generation. This flexibility presents a promising strategy for optimizing biofuel production based on desired energy outputs. In regions like India, where DWW is abundantly available and CG is an accessible byproduct of biodiesel production, this integrated approach offers a cost-effective and sustainable solution for decentralized bioenergy recovery.

Conflicts of interest

The authors declare that they have no known competing financial interests or personal relationships that could appear to influence the work reported in this paper.

Data availability

The authors confirm that the data supporting the findings of this study are available within the article. Further, the data will be made available on request.

 © 2025 The Author(s). Published by the Royal Society of Chemistry

Open Access Article. Published on 12 August 2025. Downloaded on 1/21/2026 11:52:35 PM.
This article is licensed under a Creative Commons Attribution-NonCommercial 3.0 Unported Licence.

The HPLC chromatogram of the VFAs produced during the co-digestion of DWW with CG. See DOI: https://doi.org/10.1039/d5ra04093k.

References

1 Press Information Bureau, *Government of India Milk Production in India*, https://pib.gov.in/FeaturesDeatils.aspx?NoteId=151137&reg=3&lang=1.
2 M. Gogoi, S. Banerjee, S. Pati and S. Ray Chaudhuri, *Geomicrobiol. J.*, 2022, **39**, 249–258.
3 N. Halder, M. Gogoi, J. Sharmin, M. Gupta, S. Banerjee, T. Biswas, B. K. Agarwala, L. M. Gantayet, M. Sudarshan, I. Mukherjee, A. Roy and S. Ray Chaudhuri, *J. Hazard. Toxic Radioact. Waste*, 2020, **24**, 4–10.
4 W. Han, Y. Yan, Y. Shi, J. Gu, J. Tang and H. Zhao, *Sci. Rep.*, 2016, **6**, 1–9.
5 A. K. Pandey, K. Do Park, R. Morya, H. H. Joo and S. H. Kim, *J. Environ. Manage.*, 2025, **375**, 124195.
6 Y. Yang, J. Bu, Y. W. Tiong, S. Xu, J. Zhang, Y. He, M. Zhu and Y. W. Tong, *Environ. Res.*, 2024, **244**, 117946.
7 T. R. W. Meier, P. A. Cremonez, T. C. Maniglia, S. C. Sampaio, J. G. Teleken and E. A. da Silva, *J. Cleaner Prod.*, 2020, **258**, 120833.
8 R. P. Asopa, M. M. Ikram and V. K. Saharan, *Bioresour. Technol. Rep.*, 2022, **18**, 101084.
9 Y. Bansod, B. Crabbe, L. Forster, K. Ghasemzadeh and C. D'Agostino, *J. Cleaner Prod.*, 2024, **437**, 140485.
10 T. Attarbachi, M. D. Kingsley and V. Spallina, *Fuel*, 2023, **340**, 127485.
11 P. Saila and M. Hunsom, *Korean J. Chem. Eng.*, 2015, **32**, 2412–2417.
12 C. Sivasankaran, P. K. Ramanujam, B. Balasubramanian and J. Mani, *Biofuels*, 2019, **10**, 309–314.
13 C. Zhang, D. Wu and H. Ren, *Sci. Rep.*, 2020, **10**, 2–9.
14 S. H. Kim, H. J. Kim, S. K. Bhatia, R. Gurav, J.-M. Jeon, J.-J. Yoon, S.-H. Kim, J. Ahn and Y.-H. Yang, *Korean J. Chem. Eng.*, 2022, **39**, 2156–2164.
15 C. V. Rodrigues, F. A. Rios Alcaraz, M. G. Nespeca, A. V. Rodrigues, F. Motteran, M. A. Tallarico Adorno, M. B. A. Varesche and S. I. Maintinguer, *Renewable Energy*, 2020, **162**, 701–711.
16 J. dos Santos Ferreira, I. Volschan and M. C. Cammarota, *Environ. Sci. Pollut. Res.*, 2018, **25**, 21811–21821.
17 M. S. Fountoulakis and T. Manios, *Bioresour. Technol.*, 2009, **100**, 3043–3047.
18 O. Sarkar, L. Matsakas, U. Rova and P. Christakopoulos, *iScience*, 2023, **26**(4), 106519.
19 S. Saxena, V. K. Saharan and S. George, *Ultrason. Sonochem.*, 2019, **58**, 104692.
20 B. Aylin Alagöz, O. Yenigün and A. Erdinçler, *Ultrason. Sonochem.*, 2018, **40**, 193–200.
21 S. Kumar, P. Gandhi, M. Yadav, K. Paritosh, N. Pareek and V. Vivekanand, *Renewable Energy*, 2019, **139**, 753–764.
22 A. El Nemr, M. A. Hassaan, M. R. Elkatory, S. Ragab, M. A. El-Nemr, L. Tedone, G. De Mastro and A. Pantaleo, *Ultrason. Sonochem.*, 2022, **90**, 106197.
23 S. Hashemi, P. Joseph, A. Mialon, S. Moe, J. J. Lamb and K. M. Lien, *Bioresour. Technol. Rep.*, 2021, **16**, 100874.
24 F. Ale Enriquez and B. K. Ahring, *Bioresour. Technol.*, 2024, **411**, 131330.
25 D. Young, V. Dollhofer, T. M. Callaghan, S. Reitberger, M. Lebuhn and J. P. Benz, *Bioresour. Technol.*, 2018, **268**, 470–479.
26 B. Hua, Y. Cai, Z. Cui and X. Wang, *Anaerobe*, 2022, **76**, 102603.
27 M. Nabi, G. Zhang, F. Li, P. Zhang, Y. Wu, X. Tao, S. Bao, S. Wang, N. Chen, J. Ye and J. Dai, *Desalin. Water Treat.*, 2020, **175**, 341–351.
28 Grinding matter for the UK's first biogas plant, *World Pumps*, 2008, **2008**, 12, DOI: 10.1016/S0262-1762(07)70428-5.
29 H. Warade, S. Mukwane, K. Ansari, D. Agrawal, P. Asaithambi, M. Eyvaz and M. Yusuf, *Discover Mater.*, 2025, **5**, 53.
30 R. Karray, M. Hamza and S. Sayadi, *Bioresour. Technol.*, 2015, **187**, 205–213.
31 S. Jin, G. Zhang, P. Zhang, L. Jin, S. Fan and F. Li, *Int. Biodeterior. Biodegrad.*, 2015, **104**, 477–481.
32 J. Rajesh Banu, Preethi, M. Gunasekaran, V. Kumar, S. K. Bhatia and G. Kumar, *Bioresour. Technol.*, 2022, **365**, 128164.
33 M. Chegukrishnamurthi, S. Nagarajan, S. Ravi, S. N. Mudliar and V. V. Ranade, *Commun. Biol.*, 2025, **8**, 326.
34 R. Xie, Y. Xing, Y. A. Ghani, K. E. Ooi and S. W. Ng, *J. Environ. Eng. Sci.*, 2007, **6**, 533–541.
35 A. B. Pandit, in *The Mind of an Engineer*, Springer, Singapore, 2016, pp. 329–340.
36 A. Chávez-Martínez, R. A. Reyes-Villagrana, A. L. Rentería-Monterrubio, R. Sánchez-Vega, J. M. Tirado-Gallegos and N. A. Bolivar-Jacobo, *Foods*, 2020, **9**, 1688.
37 Preethi, J. R. Banu, G. kumar and M. Gunasekaran, *Bioresour. Technol.*, 2023, **369**, 128376.
38 S. Sittijunda and A. Reungsang, *Int. J. Hydrogen Energy*, 2012, **37**, 13789–13796.
39 C. Varella Rodrigues, K. Oliveira Santana, M. G. Nespeca, A. Varella Rodrigues, L. Oliveira Pires and S. I. Maintinguer, *Int. J. Hydrogen Energy*, 2020, **45**, 11943–11953.
40 A. H. N. Armylisas, S. S. Hoong and T. N. M. Tuan Ismail, *Biomass Convers. Biorefin.*, 2023, **14**, 28341–28353.
41 A. Upadhyay, A. Chawade, M. M. Ikram, V. K. Saharan, N. Pareek and V. Vivekanand, *Processes*, 2023, **11**, 3163.
42 F. M. S. Silva, L. B. Oliveira, C. F. Mahler and J. P. Bassin, *Int. J. Hydrogen Energy*, 2017, **42**, 22720–22729.
43 E. W. Rice, R. B. Baird, A. D. Eaton and L. S. Clesceri, *Standard Methods for the Examination of Water and Wastewater*, 2012, vol. 51.
44 R. Karki, W. Chuenchart, K. C. Surendra, S. Sung, L. Raskin and S. K. Khanal, *Bioresour. Technol.*, 2022, **343**(2021), 126063.
45 Y. Li, Z. Zhang, D. J. Lee, Q. Zhang, Y. Jing, T. Yue and Z. Liu, *J. Cleaner Prod.*, 2020, **276**, 123193.
46 M. Danish, M. W. Mumtaz, M. Fakhar and U. Rashid, *Chiang Mai J. Sci.*, 2017, **44**, 1570–1582.

Open Access Article. Published on 12 August 2025. Downloaded on 1/21/2026 11:52:35 PM.
This article is licensed under a Creative Commons Attribution-NonCommercial 3.0 Unported Licence.

47 S. S. O. Silva, M. R. Nascimento, R. J. P. Lima, F. M. T. Luna and C. L. Cavalcante Júnior, *AppliedChem*, 2023, **3**, 492–508.
48 S. Kongjao, S. Damronglerd and M. Hunsom, *Korean J. Chem. Eng.*, 2010, **27**, 944–949.
49 F. M. S. Silva, C. F. Mahler, L. B. Oliveira and J. P. Bassin, *Waste Manage.*, 2018, **76**, 339–349.
50 K. Sani, S. O-Thong, R. Jariyaboon, A. Reungsang, H. Yasui and P. Kongjan, *Carbon Resour. Convers.*, 2025, **8**, 100311.
51 B. W. Gebreegziabher, A. A. Dubale, M. S. Adaramola and J. Morken, *BioEnergy Res.*, 2025, **18**, 1–25.

 © 2025 The Author(s). Published by the Royal Society of Chemistry